

Cation-Induced Synthesis of New Polyoxopalladates

Zheng-Guo Lin, Bo Wang,* Jie Cao, Bao-Kuan Chen, Yuan-Zhe Gao, Ying-Nan Chi, Chong Xu, Xian-Qiang Huang, Ruo-Dan Han, Shuang-Yue Su, and Chang-Wen Hu*

Key Laboratory of Cluster Science, Ministry of Education of China, School of Chemistry, Beijing Institute of Technology, Beijing 100081, People's Republic of China

Supporting Information

ABSTRACT: Seven polyoxopalladate compounds, $[\text{Pd}_{15}(\text{SeO}_3)_{10}(\mu_3\text{-O})_{10}]^{10-}$, with Na^+ (**1**) and K^+ (**2**) as counterions, and $\text{Na}_6[\text{M}^{\text{II}}\{\text{Pd}_{12}(\text{SeO}_3)_8(\mu_4\text{-O})_8\}] \cdot n\text{H}_2\text{O}$ ($\text{M} = \text{Co}$ (**3**), Zn (**4**), Ni (**5**), Cu (**6**), Mn (**7**); $n = 7-9$), have been prepared and characterized by SXRD, FT-IR, UV-vis, EA, TGA, and ESI-MS. These compounds comprise two distinct cluster configurations, $\{\text{Pd}_{15}\}$ and $\{\text{M}^{\text{II}}\text{Pd}_{12}\}$, which reveals the possibility of obtaining desired noble metal clusters with a certain nuclearity by using different cations as potential structural directing or template agents in synthesis. All compounds showed apparent absorptions in the visible light region, while **3** and **7** were found to show paramagnetic behavior typical of mononuclear Co^{II} and Mn^{II} complexes with zero-field splitting.

Conventional polyoxometalates (POMs) have shown great potential in catalysis and promising magnetic properties due to the scope of available building units based on early transition metals (Mo, W, V, Nb, and Ta).^{1,2} Beyond the realm of conventional transition metals, noble metals, as the active ingredients of many catalysts, find their way to lots of critical industrial applications.³ The investigation of noble-metal-containing POMs is an area of great importance and has drawn much attention in recent years.⁴⁻⁹

Several noble metal-oxygen clusters based on Pt, Pd, and Au have been synthesized.⁵ For instance, the first noble-metal-based POM $[\text{Pt}_{12}\text{O}_8(\text{SO}_4)_{12}]^{4-}$ was prepared by Wickleder and Pley,^{5a} and the palladium-based POMs have promoted the area since the first polyoxopalladate $[\text{Pd}_{13}\text{As}_8\text{O}_{34}(\text{OH})_6]^{8-}$ synthesized by Kortz et al.^{5b} Several other polyoxopalladates, $\{\text{Pd}_{13}\}$, $\{\text{Pd}_{15}\}$, $\{\text{X}^{\text{III}}\text{Pd}_{12}\}$, $\{\text{Pd}_{17}\}$, $\{\text{Pd}_7\text{V}_6\}$, and $\{\text{Cu}_2\text{Pd}_{22}\}$, bridged by PhAsO_3^{2-} , SeO_3^{2-} , AsO_4^{3-} , VO_3^- , or PO_4^{3-} , have also been reported lately.⁶⁻⁹ It is shown that the assembly of these clusters is largely affected by hydrolyzation condensation and selection of various bridging groups.⁶ However, the role of guest cations in the construction of these clusters is rather unclear, and controlled synthesis of polyoxopalladates with desired nuclearity remains challenging.

Herein, we report two $\{\text{Pd}_{15}\}$ cages comprising free guest H_2O molecules instead of metal ions with the formulas $\text{Na}_{11}\text{H}_9[\text{Pd}_{15}(\text{SeO}_3)_{10}(\mu_3\text{-O})_{10}]_2 \cdot 38\text{H}_2\text{O}$ (**1**) and $\text{K}_5\text{H}_5[\text{Pd}_{15}(\text{SeO}_3)_{10}(\mu_3\text{-O})_{10}]_2 \cdot 21\text{H}_2\text{O}$ (**2**). Moreover a new class of $\{\text{Pd}_{13}\}$ derivatives, $\text{Na}_6[\text{M}^{\text{II}}\{\text{Pd}_{12}(\text{SeO}_3)_8(\mu_4\text{-O})_8\}] \cdot n\text{H}_2\text{O}$ ($\text{M} = \text{Co}$ (**3**), Zn (**4**), Ni (**5**), Cu (**6**), Mn (**7**); $n = 7-9$), has been prepared, all of which share an identical

cubical topology ($\{\text{Pd}_{12}\}$ cage) with a unique eight-coordinated central M^{2+} cation. This, for the first time, demonstrates the controllability of polynuclearity using metal cations as the potential templating and/or structural-directing agents.

In this study, to systematically investigate the configurations of polyoxopalladates affected by different cations, we selected alkali metal cations, Na^+ and K^+ , and a handful of representative transition metal cations M^{2+} , to prepare the SeO_3^{2-} group-based polyoxopalladates. Under similar synthetic conditions, Pd^{2+} , SeO_3^{2-} , and corresponding M^{2+} were used to give two types of distinctive clusters, $\{\text{Pd}_{15}\}$ and $\{\text{M}^{\text{II}}\text{Pd}_{12}\}$, in a one-pot reaction. All clusters are stable when exposed to air over days and can be recrystallized in water. These new polyoxopalladates have been characterized by single crystal X-ray diffraction (SXRD), FT-IR, UV-vis, EA, TGA, and ESI-MS. Furthermore, the variable-temperature magnetic susceptibility of **3** and **7** was also measured.

Single-crystal X-ray diffraction analysis exhibited that **1** and **2** share a $[\text{Pd}_{15}(\text{SeO}_3)_{10}(\mu_3\text{-O})_{10}]^{10-}$ cluster shell with a pseudo-5-fold symmetry. As shown in Figure 1a, $\{\text{Pd}_{15}\}$ consists of 15

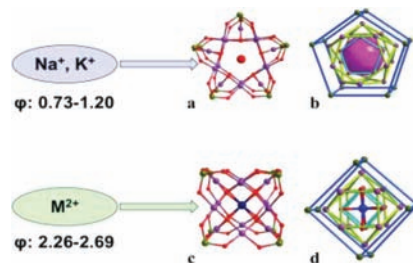


Figure 1. Ball-and-stick diagrams of $[\text{Pd}_{15}(\text{SeO}_3)_{10}(\mu_3\text{-O})_{10}]^{10-}$ and $[\text{M}^{\text{II}}\text{Pd}_{12}(\text{SeO}_3)_8(\mu_4\text{-O})_8]^{6-}$. Pd, purple; Se, deep green; O, red; M, blue ($\varphi = Z/r$; Z, charge; r, radius of the cation).

Pd atoms as the backbone and is completed by 10 SeO_3^{2-} groups. All Pd atoms are further connected by 10 internal μ_3 -oxo groups with a common square-planer geometry and are arranged in three pentagonal ABA layers. Ten out of these 15 Pd atoms serve as vertices of a pentagonal prism, while the remaining five Pd atoms sit above the center of each side face of this prism. In contrast to other polyoxopalladates with similar topology reported so far, **1** and **2** have a $\{\text{Pd}_{15}\}$ shell without any central metal ions.^{6b,7,8}

Received: February 29, 2012

Published: April 2, 2012



Compounds 3–7 have a $\{\text{Pd}_{12}\}$ shell with a general formula of $[\text{M}^{\text{II}}\{\text{Pd}_{12}(\text{SeO}_3)_8(\mu_4\text{-O})_8\}]^{6-}$. As proved by SXRD, the five clusters are isorecticular and crystallize in an orthorhombic crystal system with the space group $Pnma$. Their underlying topology is very similar to the previously reported $\{\text{Pd}_{13}\}$ clusters,^{6a} with the central Pd^{2+} being replaced by the corresponding M^{2+} (Figure 2). This central cation M^{2+} is

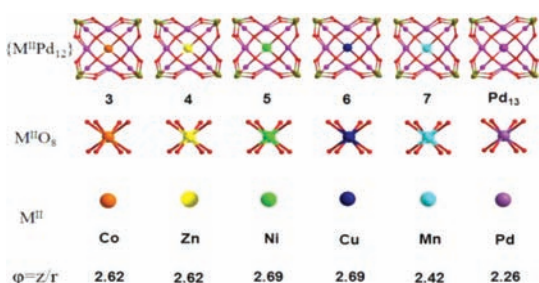


Figure 2. Ball-and-stick representation and corresponding MO_8 clusters of 3–7. The ionic potential φ of M^{2+} ions is calculated according to the eight-coordinated ionic radius in *Lang's Handbook of Chemistry*, 13th ed.; McGraw-Hill: New York, 1985.

complexed by eight inner $\mu_4\text{-O}$'s to form a pseudo-cubic body-centered constitution. The $\{\text{M}^{\text{II}}\text{Pd}_{12}\}$ cluster can be viewed as a cube with the central MO_8 cluster encapsulated by 12 Pd atoms. Each O atom in the MO_8 serves as a cube vertex and is further coordinated by three Pd atoms situated on a trigonal face of the cube. Each Pd exhibits the expected square-planar geometry by two $\mu_4\text{-O}$ and two oxygen atoms of SeO_3^{2-} . As such, 24 outer oxygen atoms form a truncated-cube-shaped shell, capped by eight selenites. Eight coordination is unusual among the first-row transition metals, since the central M^{2+} ion must be large enough to accommodate eight ligands.¹⁰ To the best of our knowledge, the transition metal M^{2+} with a cubic eight-coordinated geometry in a stable cluster is rather rare. For the first time, we have obtained a series of $\text{M}^{\text{II}}\text{O}_8$ clusters encapsulated in a $\{\text{Pd}_{12}\}$ shell. Selected $\mu_4\text{-O-M}$ bond lengths in 3–7 are shown in Table S3.

By systematically altering the cations, compounds 1–7 were synthesized in a one-pot self-assembly reaction. On the basis of structural analyses, some general synthetic principles can be derived. When only alkali cations are present, as shown in the case of 1 and 2, $\{\text{Pd}_{15}\}$ clusters tend to form upon controlled hydrolysis and polycondensation of Pd^{2+} . However, when transition metal cations, such as Co^{2+} , Zn^{2+} , Ni^{2+} , Cu^{2+} , and Mn^{2+} , are introduced, no $\{\text{Pd}_{15}\}$ is found. Instead, the shell of $\{\text{Pd}_{12}\}$ with M^{2+} encapsulated in the center is formed. It suggests that these cations may possibly serve as the structural directing agents in the formation of the targeted polyoxopalladates. Furthermore, in the case of compounds 3–7, transition metal cations also perform as the potential templating agents and help the construction of the outer shell.

A closer analysis of the ionic radius and ionic potential (φ) of the selected metal cations reveals that the ionic potential of M^{2+} in the MO_8 cuboctahedron is very close to, yet slightly larger than, that of Pd^{2+} (Pd, 2.26; Mn, 2.42; Co, 2.62; Zn, 2.62; Cu, 2.70; Ni, 2.70). As such, with similar polarity to Pd^{2+} but a smaller size, these transition metal cations can replace the central Pd ion in $\{\text{Pd}_{13}\}$ and the inductively formed cavity of $\{\text{Pd}_{12}\}$ (Figure 2). Na^+ and K^+ , on the other hand, have much smaller φ values, 1.20 for Na^+ and 0.73 for K^+ , and therefore only lead to $\{\text{Pd}_{15}\}$ clusters. This finding is also consistent with

the result of XO_8 reported in $[\text{X}^{\text{III}}\text{Pd}_{12}(\text{AsPh})_8\text{O}_{32}]^{5-}$ ($\text{X} = \text{Y}$, Pr^{3+} , etc.).⁹

In the process of SXRD data analyses and refinement of 1 and 2, Na^+ and K^+ ions, according to the known $\{\text{NaPd}_{15}\}$ structure,⁸ were originally assigned as the central atoms, respectively. However, an unusually high equivalent isotropic displacement parameter, U_{eq} , is shown.¹¹ In contrast, when O was used instead, U_{eq} fell into a normal range. Thus, to thoroughly investigate the details of 1 and 2 and determine the central atoms encapsulated, we decided to analyze the clusters in solution using ESI-MS (Figure 3a,b). These results exhibited

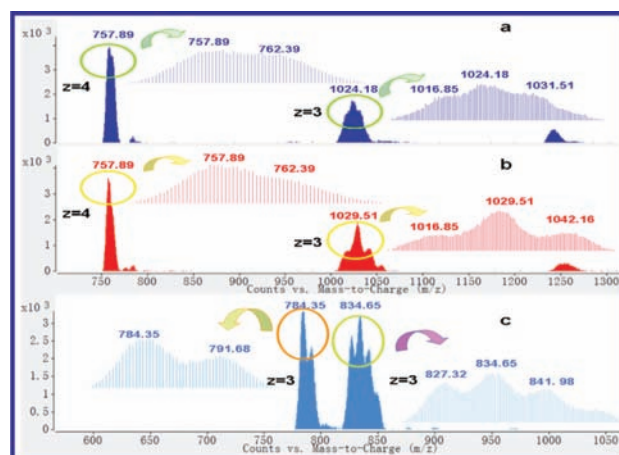


Figure 3. Negative ion mass spectra of $\text{Na}_{11}\text{H}_9[\text{Pd}_{15}(\text{SeO}_3)_{10}(\mu_3\text{-O})_{10}]_2 \cdot 38\text{H}_2\text{O}$ (a), $\text{K}_5\text{H}_5[\text{Pd}_{15}(\text{SeO}_3)_{10}(\mu_3\text{-O})_{10}] \cdot 21\text{H}_2\text{O}$ (b), and $\text{Na}_6[\text{Pd}_{12}(\text{SeO}_3)_8(\mu_4\text{-O})_8\text{Ni}] \cdot 9\text{H}_2\text{O}$ (c).

that the $\{\text{Pd}_{15}\}$ shell in both 1 and 2 indeed encapsulated a free water molecule instead of Na^+ or K^+ . For the peaks observed, $m/z = 757.89$ and $m/z = 762.39$ are present in both 1 and 2, which can be assigned to -4 charged hexaprotonated dehydrated and hydrated species, with the formulas of $[\text{H}_6\text{Pd}_{15}\text{Se}_{10}\text{O}_{40}]^{4-}$ and $[\text{H}_6\text{Pd}_{15}\text{Se}_{10}\text{O}_{40}(\text{H}_2\text{O})]^{4-}$. Unlike the Na^+ ion found in the previously reported $\{\text{NaPd}_{15}\}$ cluster,⁸ the central H_2O molecule in 1 and 2 can be readily removed, giving an empty $\{\text{Pd}_{15}\}$ shell. Despite the fact that K^+ is heavier than Na^+ and H_2O , the ionization behavior of 2 resembles that of 1 in the ESI-MS. The -3 charged peaks in both 1 and 2 observed at $m/z = 1016.85$ can be assigned to $[\text{H}_7\text{Pd}_{15}(\text{SeO}_3)_{10}(\mu_3\text{-O})_{10}\text{H}_2\text{O}]^{3-}$. In the spectrum of 1 (Figure 3a), the peaks at $m/z = 1024.18$ and $m/z = 1031.51$ can be assigned to $[\text{Na}_6\text{H}_6\text{Pd}_{15}(\text{SeO}_3)_{10}(\mu_3\text{-O})_{10}\text{H}_2\text{O}]^{3-}$ and $[\text{Na}_2\text{H}_5\text{Pd}_{15}(\text{SeO}_3)_{10}(\mu_3\text{-O})_{10}\text{H}_2\text{O}]^{3-}$. In the spectrum of 2 (Figure 3b), peaks at $m/z = 1029.51$ and $m/z = 1042.16$ will be assigned to $[\text{KH}_6\text{Pd}_{15}(\text{SeO}_3)_{10}(\mu_3\text{-O})_{10}\text{H}_2\text{O}]^{3-}$ and $[\text{K}_2\text{H}_5\text{Pd}_{15}(\text{SeO}_3)_{10}(\mu_3\text{-O})_{10}\text{H}_2\text{O}]^{3-}$. Therefore, the ESI-MS combined with elemental analyses and crystallographic data can unambiguously determine the guest molecule in POMs and solve the challenge faced in crystallography to distinguish species with same electron configuration, as in the case of Na^+ and O^{2-} .

Further, we measured mass spectra of 3–7 and confirmed the encapsulation of M^{2+} with a general formula of $\{\text{M}^{\text{II}}\text{Pd}_{12}\}$ (Figures S12–S14). For instance, in the mass spectrum of 5 (Figure 3c), the -3 charged peaks at $m/z = 827.32$, $m/z = 834.65$, and $m/z = 841.98$ can be assigned to $[\text{H}_3\text{Pd}_{12}(\text{SeO}_3)_8(\mu_4\text{-O})_8\text{Ni}]^{3-}$, $[\text{NaH}_2\text{Pd}_{12}(\text{SeO}_3)_8(\mu_4\text{-O})_8\text{Ni}]^{3-}$, and $[\text{Na}_2\text{HPd}_{12}(\text{SeO}_3)_8(\mu_4\text{-O})_8\text{Ni}]^{3-}$. Also, in the

same spectrum, we spotted some fragment peaks, $m/z = 784.35$ and $m/z = 791.68$, that can be easily assigned to $[\text{HPd}_{12}\text{Se}_7\text{O}_{29}\text{Ni}]^{3-}$ and $[\text{NaPd}_{12}\text{Se}_7\text{O}_{29}\text{Ni}]^{3-}$. This indicates that SeO_3^{2-} can be removed from the $\{\text{M}^{\text{II}}\text{Pd}_{12}\}$ during the ionization process in ESI-MS measurement, while the rest remains intact. Clearly, these fine structures in mass spectra are helpful in investigating the structural stability of such novel polyoxopalladates.

To further analyze the impact of cations on polyoxopalladate configurations, UV-vis spectra of **1**–**7** were measured in aqueous solution. Three absorption peaks are displayed in the range of 190–550 nm. Two peaks are shown in the ultraviolet region, while an apparent absorption peak emerges in the visible light region. That might bring new photocatalytic properties to POMs (Figures S5 and S6).¹² The measurements of magnetic susceptibility on **3** and **7** showed paramagnetic behavior typical of mononuclear Co(II) and Mn(II) complexes with zero-field splitting (ZFS; Figure S15).

In conclusion, by introducing various metal cations, we have synthesized seven polyoxopalladates under similar synthetic conditions. The presence of different cations plays a critical role in the formation of desired clusters and thus can potentially perform as structural directing and/or template agents. Specifically, alkali metals, such as Na^+ and K^+ , will preferably lead to $\{\text{Pd}_{15}\}$ with a free H_2O molecule inside. Meanwhile, early d-block transition metals, M^{2+} , will most likely generate $\{\text{M}^{\text{II}}\text{Pd}_{12}\}$ clusters with a corresponding M^{II} center. One possible explanation is that cations with similar ionic potentials can assist the formation of polyanion structures with the same underlying topology. In addition, we embarked on an extensive study and comparison of ESI-MS data of each compound and determined the details of the cluster structure and species inside. These results and findings shed light on the pursuit of controlled synthesis of targeted POMs, polyoxopalladates in particular, and possibly lead to the discovery of more new functional clusters. An investigation of other multiple-charged metal cations as structural directing agents is in process and will be reported.

■ ASSOCIATED CONTENT

■ Supporting Information

Experimental procedures and analysis (PDF). Crystallographic data of **1**–**7** (CIF). These material are available free of charge via the Internet at <http://pubs.acs.org>

■ AUTHOR INFORMATION

■ Corresponding Author

*E-mail: cwhu@bit.edu.cn; bowang@bit.edu.cn.

■ Notes

The authors declare no competing financial interest.

■ ACKNOWLEDGMENTS

This work was financially supported by the NSFC (20731002 and 21173021), the 111 Project (B07012), the Program of Cooperation of the Beijing Education Commission (20091739006), and Beijing Municipal Science & Technology Commission (Z09010300820902).

■ REFERENCES

(1) (a) Pope, M. T. *Heteropoly and Isopoly Oxometalates*; Springer: Berlin, 1983. (b) Yamase, T.; Pope, M. T. *Polyoxometalate Chemistry*

for Nano-Composite Design; Kluwer Academic Publishers: New York, 2002.

(2) (a) Hill, C. L. *Chem. Rev.* **1998**, *98*, 1–387 (Special Issue on Polyoxometalates). (b) Müller, A.; Roy, S. *Coord. Chem. Rev.* **2003**, *245*, 153–166. (c) Long, D. L.; Tsunashima, R.; Cronin, L. *Angew. Chem., Int. Ed.* **2010**, *49*, 1736–1758.

(3) (a) Ertl, G.; Weitkamp, J. *Handbook of Heterogeneous Catalysis*; Wiley: Weinheim, Germany, 2008. (b) Arends, I. W. C. E.; Brink, G. J. T.; Sheldon, R. A. *Science* **2000**, *287*, 1636–1639. (c) Kaledin, A. L.; Huang, Z.; Geletii, Y. V.; Lian, T.; Hill, C. L.; Musaev, D. G. *J. Phys. Chem. A* **2010**, *114*, 73–80.

(4) (a) Knoth, W. H.; Domaille, P.; Harlow, R. L. *Inorg. Chem.* **1986**, *25*, 1577–1584. (b) Bi, L. H.; Kortz, U.; Keita, B.; Nadjo, L.; Borrmann, H. *Inorg. Chem.* **2004**, *43*, 8367–8372. (c) Kurata, T.; Uehara, A.; Hayashi, Y.; Isobe, K. *Inorg. Chem.* **2005**, *44*, 2524–2530. (d) Anderson, T. M.; Neiwert, W. A.; Kirk, M. L.; Piccoli, P. M. B.; Schultz, A. J.; Koetzle, T. F.; Musaev, D. G.; Morokuma, K.; Cao, R.; Hill, C. L. *Science* **2004**, *306*, 2074–2077. (e) Villanneau, R.; Proust, A. *Eur. J. Inorg. Chem.* **2009**, 479–488. (f) Besson, C.; Huang, Z.; Geletii, Y. V.; Lense, S.; Hardcastle, K. I.; Musaev, D. G.; Lian, T.; Proust, A.; Hill, C. L. *Chem. Commun.* **2010**, *46*, 2784–2786. (g) Besson, C.; Geletii, Y. V.; Villain, F.; Villanneau, R.; Hill, C. L.; Proust, A. *Inorg. Chem.* **2009**, *48*, 9436–9443. (h) Cao, R.; Anderson, T. M.; Piccoli, P. M.; Schultz, A. J.; Koetzle, T. F.; Geletii, Y. V.; Slonkina, E.; Hedman, B.; Hodgson, K. O.; Hardcastle, K. I.; Fang, X.; Kirk, M. L.; Knottenbelt, S.; Kogerler, P.; Musaev, D. G.; Morokuma, K.; Takahashi, M.; Hill, C. L. *J. Am. Chem. Soc.* **2007**, *36*, 11118–11133.

(5) (a) Pley, M.; Wickleder, M. S. *Angew. Chem., Int. Ed.* **2004**, *43*, 4168–4170. (b) Chubarova, E. V.; Dickman, M. H.; Keita, B.; Nadjo, L.; Miserque, F.; Mifsud, M.; Arends, I. W. C. E.; Kortz, U. *Angew. Chem., Int. Ed.* **2008**, *47*, 9542–9546. (c) Izarova, N. V.; Vankova, N.; Heine, T.; Biboum, R. N.; Nadjo, B. L.; Kortz, U. *Angew. Chem., Int. Ed.* **2010**, *49*, 1886–1889.

(6) (a) Izarova, N. V.; Dickman, M. H.; Biboum, R. N.; Keita, B.; Nadjo, L.; Ramachandran, V.; Dalal, N. S.; Kortz, U. *Inorg. Chem.* **2009**, *48*, 7504–7506. (b) Izarova, N. V.; Biboum, R. N.; Keita, B.; Mifsud, M.; Arends, I. W. C. E.; Jameson, G. B.; Kortz, U. *Dalton Trans.* **2009**, 9385–9387. (c) Izarova, N. V.; Vankova, N.; Banerjee, A.; Jameson, G. B.; Heine, T.; Schinle, F.; Hampe, O.; Kortz, U. *Angew. Chem., Int. Ed.* **2010**, *49*, 7807–7811. (d) Stuckart, M. B.; Izarova, N. V.; Jameson, G. B.; Ramachandran, V.; Wang, Z. X.; Tol, J. V.; Dalal, N. S.; Biboum, R. N.; Keita, B.; Nadjo, L.; Kortz, U. *Angew. Chem., Int. Ed.* **2011**, *50*, 2639–2642.

(7) Xu, F.; Scullion, R. A.; Yan, J.; Miras, H. N.; Busche, C.; Scandurra, A.; Pignataro, B.; Long, D. L.; Cronin, L. *J. Am. Chem. Soc.* **2011**, *133*, 4684–4686.

(8) Delferro, M.; Graiff, C.; Elviri, L.; Predieri, G. *Dalton Trans.* **2010**, *39*, 4479–4481.

(9) Barsukova, M.; Izarova, N. V.; Biboum, R. N.; Keita, B.; Nadjo, L.; Ramachandran, V.; Dalal, N. S.; Antonova, N. S.; Carbó, J. J.; Poblet, J. M.; Kortz, U. *Chem.—Eur. J.* **2010**, *16*, 9076–9085.

(10) Miessler, G. L.; Tarr, D. A. *Inorganic Chemistry*; Pearson Education: London, 2003.

(11) Müller, P.; Herbst-Irmer, R.; Spek, A. L.; Schneider, T. R.; Sawaya, M. R. *Crystal Structure Refinement: A Crystallographer's Guide to SHELXL*; Oxford University Press: New York, 2006.

(12) (a) Zhang, Z. Y.; Lin, Q. P.; Zheng, S. T.; Bu, X. H.; Feng, P. Y. *Chem. Commun.* **2011**, *47*, 3918–3920. (b) Zhang, Z. Y.; Lin, Q. P.; Kurunthu, D.; Wu, T.; Zuo, F.; Zheng, S. T.; Bardeen, C. J.; Bu, X. H.; Feng, P. Y. *J. Am. Chem. Soc.* **2011**, *133*, 6934–6937.